



# Advances in the Physiology of Transvascular Exchange and A New Look At Rational Fluid Prescription

Mario E Alamilla-Sanchez <sup>1</sup>, Miguel A Alcalá-Salgado<sup>2</sup>, Beatriz Cerezo Samperio<sup>1</sup>, Pamela Prado Lozano<sup>1</sup>, Juan Daniel Díaz García <sup>1</sup>, Carolina Gonzalez Fuentes<sup>1</sup>, Martín Benjamin Yama Estrella<sup>1</sup>, Enrique Fleuvier Morales Lopez<sup>1</sup>

<sup>1</sup>Department of Nephrology, Centro Medico Nacional “20 de Noviembre”, Mexico City, Mexico; <sup>2</sup>Department of Nephrology, Hospital “Christus Muguerza”, Saltillo, Coahuila, Mexico

Correspondence: Mario E Alamilla-Sanchez, Tel +52 5541334931, Email silenoz1@hotmail.com

**Abstract:** The Starling principle is a model that explains the transvascular distribution of fluids essentially governed by hydrostatic and oncotic forces, which dynamically allow vascular refilling according to the characteristics of the blood vessel. However, careful analysis of fluid physiology has shown that the principle, while correct, is not complete. The revised Starling principle (Michel-Weinbaum model) provides relevant information on fluid kinetics. Special emphasis has been placed on the endothelial glycocalyx, whose subendothelial area allows a restricted oncotic pressure that limits the reabsorption of fluid from the interstitial space, so that transvascular refilling occurs mainly from the lymphatic vessels. The close correlation between pathological states of the endothelium (eg: sepsis, acute inflammation, or chronic kidney disease) and the prescription of fluids forces the physician to understand the dynamics of fluids in the organism; this will allow rational fluid prescriptions. A theory that integrates the physiology of exchange and transvascular refilling is the “microconstant model”, whose variables include dynamic mechanisms that can explain edematous states, management of acute resuscitation, and type of fluids for common clinical conditions. The clinical-physiological integration of the concepts will be the hinges that allow a rational and dynamic prescription of fluids.

**Keywords:** Starling principle, transvascular exchange, glycocalyx, capillary refilling, volume kinetics

## Introduction

Total body water compartments include extracellular water (EC) and intracellular water (IC). In turn, the extracellular space can be subdivided into plasma volume, interstitial and lymphatic fluid, connective and bone tissue, adipose tissue, and transcellular fluid.<sup>1</sup>

Osmotic and hydrostatic pressures move water between the EC and IC compartments and its distribution will depend on the gradient between these pressures. It is widely taught that the balance between these pressures depends on a vascular transport mechanism mediated by the classic Starling principle.<sup>2</sup> However, the observations of the last 30 years have revised the classic paradigm in which the increase in venous pressure and/or the reduction in the concentration of plasmatic proteins, would lead to the formation of edema or, on the other hand, an increase in oncotic pressure would promote reabsorption of interstitial fluid to intravascular space. Thus, in recent years the role of the lymphatic vessels, the capillary pore system and the glycocalyx have gained importance. The relevance of these findings is established in the daily clinical practice of fluid prescription. The microconstant model is a rational approach to know the fluid distribution within the body compartments, to understand the kinetics of crystalloid or colloid solution, and to evaluate the potential associated complications.

## Materials and Methods

This review was carried out by searching the medical literature in PubMed, based on the following keywords: Starling principle, revised Starling principle, transvascular exchange, fluid compartments, glycocalyx, vascular anatomy, vascular refilling, volume kinetics, pharmacokinetics of crystalloids, microconstant kinetic model. Data from studies based on theories not evaluated in clinical or experimental trials were not included.

## Review of the Vascular System and Body Compartments: Arteries, Veins, Arterioles, Capillaries, and Venules

The vascular system is made up of an extensive network of arteries, capillaries, and veins that help maintain cellular homeostasis and can be divided into two essential components: the cardiovascular and lymphatic system.<sup>3</sup>

Endothelial cells can regulate vascular tone and are involved in the inflammatory and immune response. Its cell surface is covered by a glycoprotein, the glycocalyx, which, in addition to providing an electrically charged barrier, has metabolic activity<sup>4</sup> (see below).

Despite certain anatomical differences, the blood vessels have a common histology. Anatomically we can divide them into three regions or tunica: the intima, media, and adventitia. The tunica intima is the thinnest layer, composed of a single layer of endothelial cells on a basal lamina.

The tunica media is composed primarily of smooth muscle and elastin. This layer is usually more developed in large caliber arteries. Finally, the tunica adventitia is made up almost entirely of fibroelastic connective tissue; here we also find nerve and lymphatic plexuses and the vasa vasorum, responsible for the diffusion of oxygen and CO<sub>2</sub> through the vascular walls.<sup>5</sup>

## Arterial System

Arteries are classified into elastic and muscular. Elastic arteries such as the aorta have several layers of perforated elastic membrane, which allows them to adapt to large changes in blood volume, making the flow directed to smaller caliber vessels more homogeneous. Despite this, most of the arteries are muscular arteries, and their function is to ensure the blood supply to the tissues.

The continuous arterial bifurcation gives rise to the smallest vessels of the arterial system, the arterioles, which reduce blood flow to the capillaries, vessels that connect the arterial system with the venous system. Furthermore, through different interactions of neurotransmitters and hormones, capillaries regulate the tone of arteriolar smooth muscle.

The vascular endothelium is a heterogeneous layer of specialized cells. Endothelial cells represent the first barrier for small and large molecules, cells, and pathogens. The effective area is approximately 1000 m<sup>2</sup>, with a total number of 1 to 6×10<sup>13</sup> endothelial cells.<sup>6,7</sup>

A relevant histological characteristic of capillaries is that they do not have smooth muscle; they are composed of an endothelial cell layer about 0.25 μm thick and a basement membrane surrounded by pericytes. There are three types of capillaries:<sup>7</sup>

- Continuous capillaries: the most ubiquitous, their endothelial wall and basement membrane are continuous.
- Fenestrated capillaries: they are found in endocrine organs and in the glomerulus, they have pores of 75–100 Å in diameter, which allow the free exchange of water and solutes.
- Discontinuous capillaries or sinusoids: located in specialized tissues such as hematopoietic organs, they have large pores of 1500–2500 Å that allow cell exchange between blood and tissues.

Blood return to the heart through the venous system begins in the postcapillary venules, which coalesce to form larger veins. The transition from capillaries to veins is given by the reappearance of smooth muscle in the tunica media.

## Venous System

The veins branch out forming plexuses, especially in the skin and pelvic region. The intima of the great veins folds forming valves that ensure unidirectional blood flow. These valves are particularly abundant and important in the pelvic limbs. Hydrostatic pressure decreases along the arterioles and capillaries from 15 mmHg in the venules to 5–6 mmHg in the intrathoracic veins. The pressure in the right atrium, where the blood from the cavas arrives, is called central venous pressure and is approximately 4–5 mmHg. Its value depends on venous return, respiration, and the pump function of the right ventricle.<sup>8</sup> The mean systemic filling pressure is thought to remain relatively constant irrespective of the cardiac output, usually about 2–10 mmHg, very small compared to the mean arterial pressure 70–100 mmHg, relative to the thin wall of the veins.

The wall of the venules is formed by a layer of endothelial cells, surrounded by some fibroblasts. Smooth muscle is present in veins from 8 to 10 mm in diameter. The muscular middle layer is present in the veins of the pelvic limbs and is responsible for venous tone or vasomotricity.

Veins have a larger diameter than their accompanying artery, so the venous flow is slower, in the vena cava it is 7–10 cm/sec, while in the aorta it is 25–35 cm/sec. Veins are up to 10 times more distensible, so an increase in blood pressure allows more blood to be stored in the venous bed. This allows veins smaller than 1mm in diameter to store up to 65% of circulating blood; the heart (10%), systemic arteries (10%), and pulmonary circulation (10%) contain 30% of the blood volume. The capillaries only contain 5% of the circulating blood and the rest is found in the arterial system. That is, the veins are capacitance vessels and act as blood reservoirs.<sup>9</sup>

## Lymphatic System

We must always consider the lymphatic system, responsible for the transport of interstitial fluid (ISF), composed of afferent lymphatic vessels, nodes, and efferent lymphatic vessels. The thoracic duct is the largest lymphatic vessel, ultimately pumping fluid back into the systemic circulation. It is a complex and dynamic system composed of up to 10 billion capillary beds, continuously fluctuating between its perfused and collapsed state under the influence of systemic and local factors.<sup>10,11</sup> It maintains tissue homeostasis by interstitial transport of fluid, lipids, and metabolic waste products from tissues to the main circulation, in addition to having an essential role in the presentation of antigens to antigen-presenting cells in local lymph nodes.<sup>10</sup>

The initial lymphatic capillaries (ILCs) consist of a monolayer of “oak-leaf” shaped non-fenestrated lymphatic endothelial cells (LECs), lacking a basement membrane and pericytes. They are linked through discontinuous “button” junctions formed by cadherin-5, occludin, claudin-5, zonula occludens-1, selective endothelial cell adhesion molecule, and type A junctional adhesion molecule. The junctions overlap the opposing cell membranes creating “flaps”, which function as primary lymphatic valves that ensure unidirectional lymphatic movement.<sup>11</sup>

The precollecting lymphatic vessels transfer lymph from the ILCs to the collecting lymphatics. They have an additional feature: bicuspid intraluminal secondary valves that resemble those of the larger collecting vessels. Some precollecting lymphatic segments have a layer of lymphatic muscle cells (LMCs), which contract spontaneously, facilitating the transfer of lymph to the collecting lymphatic vessels. The precollector lymphatics achieve both the absorption and the propulsion of the lymph.<sup>12,13</sup>

The collecting lymphatics have an intima, media, and adventitia, and are structurally adapted to propel lymph but cannot absorb circulating interstitial fluid.<sup>14</sup>

The segmented chambers located between the valves are called “lymphangia”. The *lymphangia* are active units of lymphatic collecting vessels, which perform rhythmic contractions, essential for the propulsion of the lymph.<sup>15</sup>

The lymphatics drain the lymph back into the circulatory system via the pumps of the thoracic duct and the right lymphatic duct, into the left and right subclavian veins, respectively.<sup>16</sup>

The lymphatics handle approximately 8 liters of fluid per day, the collection of which depends on the metabolic, structural, and mechanical properties of the different tissues. Thus, the process of lymph formation is a crucial event that prevents ISF accumulation and maintains tissue homeostasis. Lymphatic capillaries normally collapse under physiological conditions; however, as the ISF accumulates in the tissue because of leaking from the blood capillaries, the pressure

of the ISF increases around the ILCs. The expanded tissue increases the tension exerted on the anchoring strands, which pulls on the strands and opens the junctions of the overlapping LECs.<sup>14</sup>

## Glycocalyx

As mentioned above, the vascular wall is commonly described as having 3 layers: tunica adventitia (connective tissue and vasa vasorum), tunica media (vascular myocytes), tunica intima (endothelial cells interconnected by tight junctions, the subendothelial space, and the internal elastic membrane).<sup>17</sup> However, the observable effect by intravital microscopy showed that the blood cells did not touch the vascular wall, initially attributable to the Fahraeus-Lindquist effect (directly proportional relationship between blood viscosity and blood vessel diameter, due to the central distribution of erythrocytes in laminar flow). However, electron microscopy and confocal microscopy revealed the presence of a fourth layer in the vascular wall: glycocalyx.<sup>18,19</sup>

The glycocalyx is composed of chains of negatively charged sulfated glycosaminoglycans (GAGs) anchored to a protein core forming proteoglycans (PGs). The main sulfated GAGs include heparan sulfate (50–90%), dermatan sulfate, and chondroitin sulfate. Also, hyaluronic acid (non-sulfated GAG) is an important constituent. Sulfated proteoglycan (syndecan 1–4 and glypican-1) are the most important core proteins of heparan sulfate.<sup>20</sup> Furthermore, sialoproteins are an important structural part of the glycocalyx, containing numerous neuroaminic acid residues.

The glycocalyx has a thickness of between 200 and 400 nm and a total volume of approximately 700 mL, it interacts intensely with plasma molecules, favoring the adsorption of molecules such as albumin and orosomucoid through electrostatic interactions,<sup>21,22</sup> in addition to participating in vascular permeability, coagulation, thrombosis, mechanotransduction and mediation of the inflammatory state.<sup>22</sup>

The glycocalyx can contribute up to 60% of the intravascular oncotic pressure.<sup>23</sup> From the perspective of the pore-based model of vascular permeability, the most accepted anatomical model of the glycocalyx is made up of periodic clusters with 10–12 nm fibers, with 20 nm inter-fiber spacing and hexagonal conformation with a center of GAGs anchored to a band of actin on the endothelial cell surface and a distance between each anchor of 100 nm.<sup>24</sup> With this model, the radius of the fiber and the inter-fiber space is what makes up the “pore size”, while the length and frequency of the GAGs-actin anchors determine the “pore density”.

The loss of glycocalyx mediated by fluid resuscitation in septic patients is favored by the degradation and release of heparan sulfate into the circulation and is associated with mortality in hospitalized septic patients.<sup>25</sup>

## Hemodynamic Forces and Transvascular Flow

The endothelium is exposed to various hemodynamic forces: radial (intravascular pressure), tangential (cell–cell interaction), and axial (shear stress due to friction between the blood and the vascular wall).<sup>6</sup> Due to the radial force, the hydraulic pressure ( $P_c$ ) is produced.

In vitro, the endothelial cell is exposed to constant or pulsatile unidirectional shear stress, from 1 to 100 dynes/cm<sup>2</sup>, which also adopts an anti-inflammatory, antithrombotic and antiproliferative phenotype. Fluid shear stress (FSS) is the tangential vector of the force exerted by blood flow and is defined as the frictional force of blood flow per unit area parallel to the vessel walls. Arterial wall is currently considered to be elastic, inhomogeneous, and anisotropic, with different mechanical properties in different directions, which confers a particular response in each segment to FSS.<sup>26</sup> The reported FSS depends on the vascular area (Table 1).<sup>27</sup>

**Table 1** Hemodynamic Factor According to Vascular Area

Component	Artery	Vein	Capillary
Wall shear stress	Aorta: 10–40 dynes/cm <sup>2</sup> Coronary arteries: 10–17 dynes/cm <sup>2</sup>	1–5 dynes/cm <sup>2</sup> Long saphenous vein: 0.5–4 dynes/cm <sup>2</sup>	Highly variable depending on vascular bed: 1–70 dynes/cm <sup>2</sup>

Among the factors that influence the sensing of shearing forces are the intercellular junctions (cadherin, PECAM-1), ion channels, tyrosine kinase receptors (VEGFR2), caveolae, actin filaments, nesprins, the primary cilium, the integrins and glycocalyx.<sup>28–34</sup>

## Classical Model of the Starling Principle

Fluid transport within the different extracellular compartments is regulated by hydraulic and oncotic pressures operating along the microvascular walls. Under normal conditions, the balance of forces across the microvasculature favors the flow of fluid from the intravascular space into the interstitium, a phenomenon known as capillary filtration. This transcapillary flow (fluid accompanied by macromolecules) can be conducted towards the lymphatic system and from there again towards the systemic circulation; the only way to restore the macromolecules (proteins) filtered into the interstitium is by draining into the lymphatic system. A lymphatic turnover of approximately 8 liters per day has been estimated, that is, a turnover of the total volume of plasma approximately every 8 hours.<sup>35</sup> Alteration of any of the forces involved can promote the accumulation of fluid, usually in the interstitium. The basis of the mechanism is the difference between the hydrostatic pressure and the plasma/interstitial oncotic pressure.

Starling's classic study involved injecting saline into the hind legs of anesthetized dogs, the fluid was absorbed directly into the blood, whereas plasma injected into the tissues was not absorbed.<sup>36</sup> This phenomenon led Ernest Starling to deduce that capillaries and post-capillary venules act as semi-permeable membranes that reabsorbed fluid from interstitium to intravascular. Landis, in 1930, measured the pressure of the capillaries of the nail bed at level of the heart: 35–45 mmHg in arterioles and 12–15 mmHg in venules;<sup>37</sup> the estimated oncotic pressure in humans is 25–28 mmHg, so the pressure difference favors transcapillary filtration in arterioles, while the lower hydrostatic pressure compared to plasma oncotic pressure in venules favors fluid reabsorption.

Another determining factor is the Staverman reflection coefficient,  $\sigma$ , whose value ranges from 0 to 1, with 1 being a solute without permeability from one compartment to another.

The currently most accepted equation based on the Starling hypothesis is expressed:

$$J_v/A = L_p([P_c - P_i] - \sigma[\pi_p - \pi_i]) = L_p(NFP)$$

Where,  $J_v/A$  = filtration flow over permeability surface area;  $L_p$  = coefficient of permeability;  $P_c$  = capillary hydrostatic pressure;  $P_i$  = interstitial hydrostatic pressure;  $\sigma$  = Staverman reflection coefficient;  $\pi_c$  = capillary oncotic pressure;  $\pi_i$  = interstitial oncotic pressure; and NFP = net filtration pressure. A positive  $J_v/A$  or NFP value is equivalent to net filtration when the value of  $J_v/A$  or NFP is negative, the opposite occurs (net reabsorption). Since the value of  $\sigma$  is approximately 0, the formula is often simplified:

$$J_v = ([P_c - P_i] - [\pi_p - \pi_i]) = NFP$$

The general view of this fluid transvascular kinetics is known as Starling principle. Its impact on clinical models was essential for understanding the pathogenic pathways of edematous disorders and the administration of parenteral solutions.

The contributions of Landis, Pappenheimer and Soto-Rivera,<sup>38–40</sup> with the integration of the pore model, favored the popularity of the Starling principle in clinical physiology.

The potential applicability of the Starling principle was greater with the advent of isoosmotic and hyperosmotic albumin in the management of patients in the resuscitation phase due to hypovolemia.<sup>41</sup>

The theory was plausible: hyperosmotic albumin bolus could raise  $\pi_p$  in such a way that it would have to favor the redistribution of fluid from interstitium to intravascular space, which should be reflected in improved mortality rates in hypovolemic patients. However, in a pediatric population study conducted in Africa, bolus of albumin showed no advantage over isotonic saline, and continuous fluid replacement was better than bolus.<sup>42</sup> The SAFE research group also did not show an advantage with the administration of albumin 4% or saline 0.9% in the resuscitation of 6997 patients: on the fourth day, the volume of both solutions was identical, and except for serum albumin concentrations, there was no difference at 28 days in days of hospitalization, days of invasive mechanical ventilation, days in renal support therapy or mortality.<sup>43</sup> Also, pharmacokinetic experiments have shown that the volume of distribution of crystalloid solutions (0.9%

saline, Ringer's lactate-acetate) is much lower than expected for the calculated extracellular volume.<sup>44</sup> Therefore, there must be additional hemodynamic mechanisms of transvascular flow, which contribute to the poor clinical outcome in conditions in which the Starling principle should have good performance.

## Revised Model of the Starling Principle

Research over the last 30 years has shown that the Starling principle is partially correct. Adamson et al<sup>45</sup> showed that the effect of  $\pi_i$  on transcapillary filtration is much less than that predicted in the standard Starling equation. In an elegant study, they evaluated the effect of the effective oncotic pressure difference ( $\sigma\Delta\pi$ ), which opposes filtration from plasma, by perfusing rat mesenteric microvessel with albumin and with or without albumin in the interstitium;  $\sigma\Delta\pi$  was shown to be almost 70% of the plasma oncotic pressure when the interstitial albumin concentration was equal to plasma. This study proposed that the ultrafiltrate that crosses the endothelial glycocalyx through the tight junctions reduces the diffusive flow of albumin from the interstitium, causing  $\sigma\Delta\pi$  to be greater than that measured between the vascular lumen and the interstitium.<sup>45</sup>

Starling principle states that at constant plasma volume, an equilibrium must exist, where  $J_v = 0 = \Delta P = \sigma\Delta\pi$ , or steady state (Figure 1). That is, absence of transvascular filtration due to the balance of hydrostatic and oncotic pressures.<sup>36</sup> However, this phenomenon does not occur in vivo for more than a fraction of a second, since the absence of filtration will cause dissipation of  $\pi_c$  due to the movement of proteins towards the interstitium. Steady state, and protein concentration, can be achieved by constant low filtration rates since water and small solutes filter through the interstitium much faster than macromolecules; these discrete changes of  $J_v$  adjust the  $\Delta\pi$  to a new steady state value.

The glycocalyx allows an ultrafiltrate with only a few macromolecules due to its high value of  $\sigma$  ( $> 0.9$ ), so the protein concentration in the ultrafiltrate will be lower than in the plasma, so the higher the transvascular filtration, the lower the protein concentration in the ultrafiltrate.<sup>46</sup> So, there is no equilibrium ( $J_v = 0 = \Delta P = \sigma\Delta\pi$ ), but a real difference in steady-state pressures.

Solute movement are another important factor of transvascular flow. Typically, Fick's first law is used for the evaluation of diffusive solute transport:

$$J_s = -D(\Delta C/\Delta X)$$

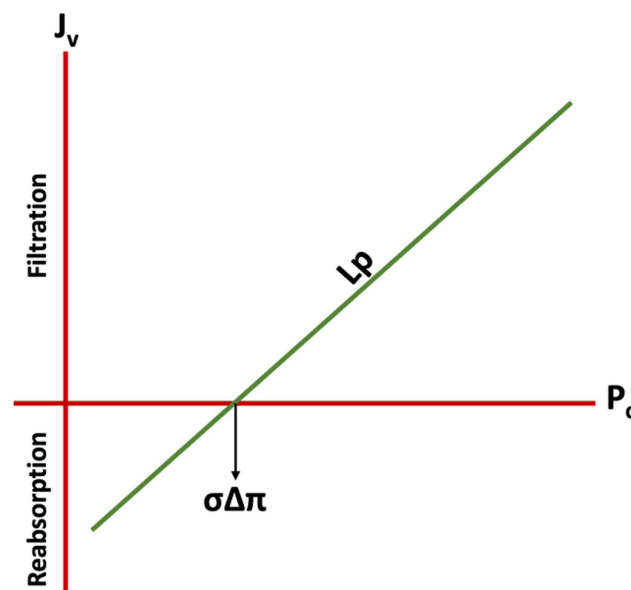


**Figure 1** Classical Starling principle. Relationship between transvascular flow ( $J_v$ ) and hydrostatic pressure ( $P_c$ ); when  $J_v = 0$ , the hydrostatic and oncotic pressure difference of the intravascular and interstitial space reach an "equilibrium" ( $\Delta P = \sigma\Delta\pi$ ), which results in the absence of vascular leakage. When  $P_c < \sigma\Delta\pi$  there is fluid reabsorption.

where  $J_s$  = diffusive flow;  $-D$  = diffusion coefficient, which in turn depends on the size of the molecule, the temperature, and the viscosity of the solvent;  $\Delta C/\Delta X$  = solute concentration gradient on both sides of the filtration barrier. Therefore, a passive type of solute transport is established due to the concentration difference of a solute on both sides of the endothelial barrier. However, water and solutes are usually transported together through the capillary, by a convective mechanism, in which the value of  $\sigma$  is not equal to 1. If the movement of solvent is increased by an increase in hydraulic pressure, therefore, there will also be an increase in the movement of solutes, a phenomenon known as “solvent drag”. This results in a “J-line” transport, not a “straight line” (zero slope) as assumed in Fick’s first law. The measurement of the relative importance between both transport mechanisms (diffusion and convection) can be correlated by means of the Péclet number ( $Pe'$ ). When the value of  $Pe' < 0.2$ , the diffusive transport is greater than the convective; when  $Pe'$  is  $> 5$ , convective transport is greater than diffusive transport.<sup>47</sup>

The validity of the  $P_c$  value has a history that challenges initially accepted calculations in vascular physiology. Levick et al<sup>48</sup> calculated the value of  $P_c$  under conditions where  $J_v = 0$  (assuming  $\sigma = 1$ ) and compared their calculations with the values of venous pressure ( $P_v$ ) obtained from previous studies performed in 14 tissues, showing that in 11 of 14 tissues, the  $P_c$  value was substantially lower (2 to 10 mmHg) compared to  $P_v$ , except in postglomerular tissue of renal cortex and medulla and in intestinal mucosa. Interestingly, in intestinal mucosa in a “non-absorbing” state,  $P_v > P_c$  by 4mmHg.

Michel et al<sup>49</sup> showed that under conditions where  $P_c < \pi_p$ , there is an expected reabsorption, this phenomenon only occurred transiently, suggesting that the effect could be explained by a gradual increase in  $\pi_i$ .

In Landis’s experimental model, it was observed that in the arterial half of the capillary at the level of the heart, where  $P_c > \Delta\pi$  (25 to 28 mmHg), there should be filtration, which is subsequently balanced by reabsorption in the venular region, where  $P_c < \Delta\pi$ .<sup>50</sup> However, Levick and Michel demonstrated that tissue flow cannot be maintained  $> 10$  cm below the level of the heart, because at the venular level  $P_c > \Delta\pi$  and there is no fluid reabsorption,<sup>50</sup> an effect that does not occur with capillaries above the heart, as the collapse of the veins reverses the pressures ( $P_c < \Delta\pi$ ).

Subsequently, Michel et al,<sup>49</sup> in a classical 2-step experiment, demonstrated the relationship between the pressure gradient and transvascular filtration. In the first model (transient state),  $P_c$  was suddenly reduced and transvascular leakage was assessed immediately. In this first phase of the experiment, it was shown that, as expected, there was a linear relationship between  $J_v$  and  $P_c$ , with a transient phase of fluid absorption when  $P_c < \sigma\Delta\pi$ . However, in the second experimental model, the  $P_c$  remained constant for at least 2 minutes or more before the leakage was measured (steady state). In this phase of the experiment, when  $P_c > \sigma\Delta\pi$ , filtration increased linearly as  $P_c$  increased, however, when  $P_c < \sigma\Delta\pi$ , the expected fluid reabsorption was not observed (Figure 2). This phenomenon can be explained with the connection between

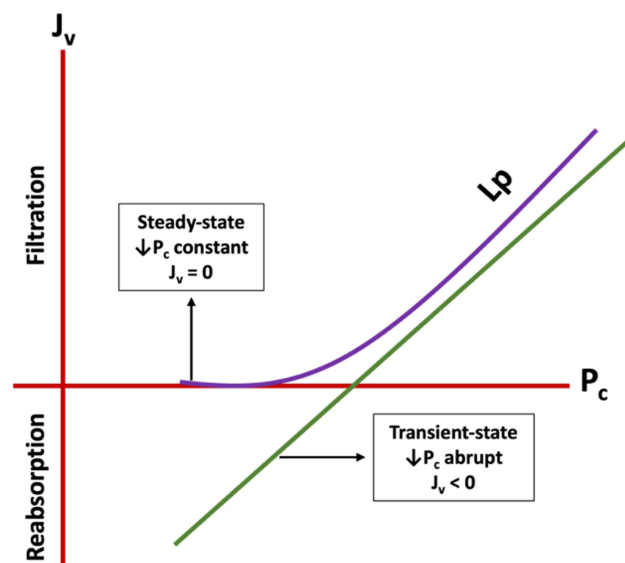


**Figure 2** Revised Starling’s principle. In the transient state with abrupt reduction of  $P_c$  (green line),  $J_v < 0$  when  $P_c < \sigma\Delta\pi$  and there is fluid reabsorption. In the steady state with constant maintenance of  $P_c$  (purple line),  $J_v = 0$  when  $P_c < \sigma\Delta\pi$  contrary to the expected reabsorption.

the concentration of proteins in the interstitium ( $\pi_i$ ), in the subglycocalyx space (see below), and the rate of vascular filtration.

The differences between the transient and steady state values of  $J_v$  are increasingly larger as  $\Delta P \ll \sigma \Delta \pi$ ; however, this difference is smaller as  $\Delta P \gg \sigma \Delta \pi$  (Figure 2).

This perspective obtained from the evidence has modified classic Starling formula:

$$J_v/A = L_p([P_c - P_i] - \sigma[\pi_p - \pi_g]) = L_p(NFP)$$

where  $\pi_g$  is the oncotic pressure in the subglycocalyx region, substituting the interstitial pressure, which explains the steady state phenomenon.

## Brief Physiology of Glycocalyx

The glycocalyx contains sulfated glycosaminoglycans (heparan- and chondroitin-sulfate) attached to proteoglycans (syndecan 1–4 and glypican-1), non-sulfated glycosaminoglycans (hyaluronic acid), oligosaccharide/sialic acid-bearing glycoproteins, and adsorbed proteins.<sup>20</sup>

At least three functions of the glycocalyx are essential for endothelial homeostasis: it functions as a mechanosensor-mechanotransducer, a mechanical barrier to blood flow, and a hydraulic regulatory barrier (vascular permeability).<sup>51</sup> These factors have a direct impact on erythrocyte mechanics in the vascular lumen, regulation of hematocrit, transmission of shear forces across the endothelium, and modulation of transvascular oncotic pressure difference. In an experimental model, Adamson et al observed that removal of 150 nm glycocalyx from frog endothelium can increase vascular permeability two-fold.<sup>52</sup>

Each anatomical component of the glycocalyx is essential for the maintenance of the endothelium. Sulfated GAGs may act as co-receptors for endothelial cell growth agents, cation scavengers, and precursors for nitric oxide synthesis. Glipican-1, linked to heparan sulfate, is a protein anchored to glycosphosphatidylinositol (GPI) that can be found in a zone of high mobility (lipid rafts) and in a fixed zone where the caveolae are located.<sup>53,54</sup> The formation of caveolae depends on the phosphorylation of caveolin-1 induced by hyaluronic acid (HA). Individual HA fibers adhere to their membrane-bound receptors, CD44 and receptor HA-mediated motility (RHAMM);<sup>55,56</sup> some portion of the HA bound to CD44 is internalized into caveolae,<sup>57</sup> which can fuse with caveosomes and represent an important pathway of transcytosis for molecules such as albumin.<sup>58,59</sup> In addition, CD44 produces activation of the sphingosine-1-phosphate receptor-1 (S1P1), stabilizing the endothelial actin network, contributing to the stability of the endothelial matrix. Sphingosine-1 phosphate (S1P) is a protective protein against glycocalyx detachment and induces its synthesis in response to chemokines (IL-8, CXCR1, CXCR2).<sup>60–62</sup>

The plasma microenvironment produces changes in the glycocalyx structure. For example, removal of plasma proteins reduces the thickness of the glycocalyx due to an increase in the influx of calcium into the endothelial cell; likewise, the high concentrations of calcium near the actin bands of the endothelium weaken their adhesion junctions, which contributes to increased vascular permeability.<sup>63,64</sup>

Oberleithner has carried out multiple experiments to study the effect of sodium on glycocalyx composition. Using nanoindentation and atomic force microscopy (AFM) techniques to estimate glycocalyx stiffness and thickness, Oberleithner et al, demonstrated that human umbilical artery cells chronically exposed (5 days) to a high sodium microenvironment (150mM) reduced the heparan sulfate expression by 68% compared to low sodium concentrations (135 mM), with a 50% collapse of the glycocalyx thickness (basal: 400 nm) and an increase in stiffness of 130% (basal: 0.25 pN/nm). Sodium overload favors cell permeability to sodium by increasing expression of the epithelial sodium channel (ENaC),<sup>65</sup> which induces a high transcellular transport, which associated with endothelial damage, leads to a delay in the renal excretion of sodium. All the phenomena that affect the thickness and/or rigidity of the glycocalyx will also alter the cell–cell interaction. Particularly, the glycocalyx of the erythrocyte membrane has an electrostatic repulsion force with the endothelium due to the negative charges on the surface of the glycocalyx,<sup>66</sup> deterioration of the glycocalyx in both cells causes an increase in shear stress that worsens endothelial damage.

## Glycocalyx and Transvascular Exchange

Despite studies demonstrating the validity of the Starling principle in general, research on the structural basis of the filtration barrier established the critical role of the glycocalyx endothelial layer, reevaluating the classic Starling Principle and proposing a revised model that it does not replace the classical theory but complements it. Further observations of the model emphasize the crucial role of the glycocalyx in transvascular transport. The adsorptive capacity of the endothelial glycocalyx for macromolecules such as albumin, orosomucoid, and lumican<sup>67</sup> provides the structure with a size- and charge-selective, semi-permeable endothelial barrier.<sup>68,69</sup> Due to their molecular structure and charge, only some macromolecules can cross the barrier.

Michel and Weinbaum hypothesized that the oncotic forces that oppose transvascular filtration are localized throughout the glycocalyx. As it was commented in the previous section, the transient state was well coupled to the premises established by Starling, however with the sustained fall of  $P_c$  and when obtaining a new stationary state, it was not found the expected effect, and no leakage occurred despite  $\Delta P < \sigma \Delta \pi$ . This leads to the conclusion that there is no global concentration difference between the plasma and the interstitium of the tissue, which must be exerted by some structure within the capillary, that is, the glycocalyx.

Undoubtedly, the ultrastructure of the interendothelial junction and the glycocalyx provides relevant information about the fluid balance determined by the concentration difference across the glycocalyx and maintained by a protected or “exclusion” zone between the glycocalyx and the interendothelial junctions (see Figure 3) which can adsorb macromolecules, mainly albumin.

## Glycocalyx–Albumin Interaction as a Regulator of Transvascular Transport

Albumin, synthesized exclusively by the liver, is the most abundant protein in the circulation and since it is smaller than most plasma proteins, its relative concentration is higher in the interstitial fluid, due to the screening characteristics of the endothelial barrier for proteins. Ten grams per day are produced with a turnover rate of 25 days. Its elimination is mainly catabolism (85%), hepatic (10%) and renal (5%) clearance.<sup>70</sup> Its molecular weight is 66 kD with a diameter of 7 nm, and it has a great capacity to fix cations such as sodium, which doubles its osmotic activity compared to other proteins (Gibbs-Donnan effect).<sup>71,72</sup> Thus, albumin in the interstitium exerts a strong impact on tissue oncotic pressure (approximately 80%), so that in states of hypoalbuminemia, the increase in other plasma proteins does not compensate

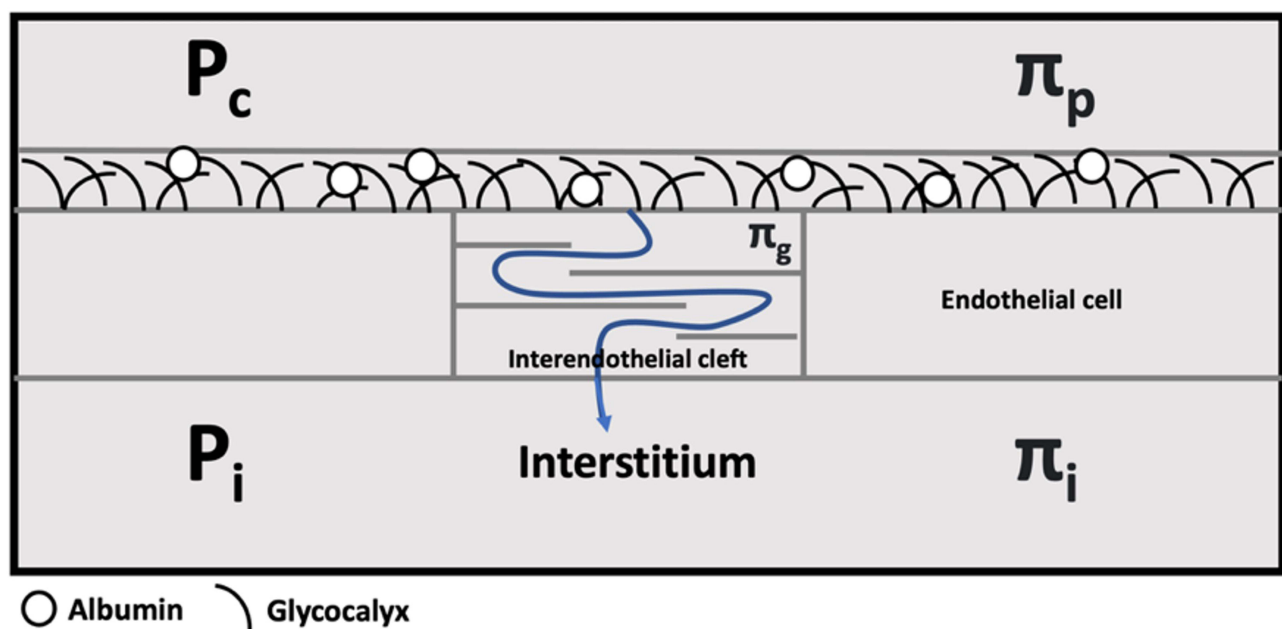


**Figure 3** Interendothelial space and clefts. The revised model of the Starling Principle proposes the glycocalyx as a major determinant in the maintenance of the  $\Delta \pi$  in the face of changes in  $P_c$ . The arrow indicates the path of flow of solvent and solutes through the interendothelial cleft.

intravascular oncotic pressure.<sup>70</sup> Interestingly, there is controversy regarding hypoalbuminemia as the generation of tissue edema in conditions such as nephrotic syndrome since it has been shown that oncotic pressure in conditions of analbuminemia does not produce the expected degree of edema.<sup>73,74</sup> Accelerated hypoproteinemia, as in experimental models in dogs, does not lead to intravascular volume deficit or activation of the renin-angiotensin-aldosterone axis.<sup>75–77</sup>

Other relevant functions include antioxidant effects, and it facilitates the transport of a wide variety of substances, due to the presence of many charged groups on the surface and ionic and hydrophobic binding sites. These substances include water, cations, free fatty acids, phospholipids, bilirubin, hormones, metabolites, metalloporphyrin ions, drugs, among others. Albumin can also be pinocytosed in cells, providing amino acids to cells after catabolism.<sup>78</sup>

Since the glycocalyx “creates” an exclusion region between the plasma and the endothelium, there is no contact of cellular components with the endothelial cell layer. This exclusion region prevents the contact of proteins >70 kDa and is the reason why albumin is one of the few proteins that can move between the plasma and the endothelium, and although its paracellular movement is very limited, there is evidence that transcellular transport (transcytosis) mediated by caveolae is one of the main transport mechanisms towards the interstitium under physiological conditions,<sup>79</sup> although not the only one, as it has been shown, in a caveolin-1 knock-out mice model, that even in the absence of transcytosis, albumin could be identified in the interstitium, probably due to an increase in compensatory paracellular transport.<sup>80</sup> Perhaps one of the physiological effects of transcytosis is the transport of molecules attached to albumin, such as fatty acids, cholesterol, and phospholipids, which in states of hypoalbuminemia and nephrotic syndrome usually increase in serum.<sup>81–83</sup>

As mentioned above, the glycocalyx represents a barrier to macromolecules in the healthy endothelium. However, it has been shown that under inflammatory conditions, as in the study by Henry et al, who carried out a protocol where they administered TNF- $\alpha$  into the hamster cremaster microvasculature, and found that 70, 580 and 2000 kDa fluorescein isothiocyanate (FITC) labeled dextrans, which are normally found in the “exclusion zone” within the vascular lumen, can permeate into the damaged glycocalyx; the same occurred with FITC-Dextran 40, FITC-albumin and FITC-IgG.<sup>84</sup> Thus, this evidence suggests redistribution of macromolecules in the vascular lumen and potentially moving oncotic forces into the subglycocalyx space ( $\pi$ g). Under what conditions this can explain the generation of accelerated edema in hospitalized patients with maintenance solutions for long periods is a question that should be investigated.

As mentioned in the previous section, the removal of plasma proteins alters vascular permeability associated with the influx of endothelial calcium and the alteration of actin binding.

## Transvascular Refilling

When the intravascular volume is decreased, a microvascular absorption of fluid from the tissues occurs combined with the lymphatic flow (composed of the partial reabsorption of the afferent lymph from the lymph nodes and the venous drainage of the afferent lymph); These events constitute the so-called vascular refilling, which is not directly measurable by clinical methods and is inferred by mathematical models.<sup>85,86</sup>

The capillaries, the area of the circulatory system that connect veins and arteries, is the area where the exchange of substances between plasma and tissues occurs. Water-soluble molecules can diffuse through the capillary pores, establishing a Gibbs Donnan equilibrium between the plasma and the interstitium. In the model proposed by Starling, it was thought that the oncotic and hydrostatic forces caused the liquids to leave the arteriolar end and return to the venular end, leaving the lymphatic vessels as escape areas due to the leakage of proteins from the capillaries; however, lymphatic flow and interstitial osmotic pressure have been found to be greater than previously thought, and lymphatic vessels play a greater role in maintaining the plasma–interstitium balance (see above).

Fluid movement between the plasma and the interstitium is influenced by the properties of the capillary wall and the pressure gradients across the membrane. Furthermore, lymph flows at a constant rate from the interstitium to blood vessels.

Research on transvascular refilling is based on various models. Bleeding produces erythrocyte dilution due to a volume expansion produced by the repletion of the volume lost during bleeding, which can be up to 90% in the first 12 to 24 hours.<sup>87,88</sup> An effect described by Cope et al is the importance of the albumin returned to the intravascular from the thoracic lymphatic duct.<sup>89</sup> Wasserman et al corroborate the plasmatic refilling of albumin through the thoracic duct, the movement of albumin masses being much greater from the ISF to the intravascular than vice versa during the first post-bleeding day; an accelerated albumin anabolism associated with reduced protein catabolic rate also contributes in

the first 2 to 5 days after plasma volume repletion.<sup>90</sup> Another study carried out in a hemorrhage model in dogs, showed that the reabsorbed fluid corresponds to 30% of the total plasma volume at the peak of the hemorrhage and reaches 60% of the total plasma volume almost at the end of the evaluation.<sup>91</sup> In the experimental model, controlled bleeding of up to 50 mL/min caused a volume loss of 30–35 mL/kg, with a transvascular refill of up to 20 mL/kg during the first hour, the same volume was obtained at 120 minutes when the bleeding rate was low (10 mL/min).<sup>91</sup> The most important sites of fluid recruitment occur in skeletal muscle and skin due to their high body surface area (40% of total body weight) containing up to 5 L of ISF and 14 L of ICF.

As previously mentioned, in Michel's experimental tests, it was shown that in the postcapillary venules of the mesentery of frogs and rats there was no significant fluid reabsorption except for a very short and limited time.<sup>49</sup>

Another model to evaluate transvascular refilling has been hypothermia. During the decrease in temperature, Nose et al demonstrated a progressive decrease in plasma volume until reaching 93% compared to controls, while the oncotic pressure was 103% compared to the control value.<sup>92</sup> Previously, Chen et al observed a bimodal effect when they monitored thoracic duct lymph flow during hypothermia (25°C) in splenectomized dogs. They demonstrate a decrease in plasma volume accompanied by an increase in lymphatic flow in the first cooling period, probably secondary to the increase in blood pressure induced by activation of the sympathetic nervous system; subsequently, a secondary decrease was observed, in the late cooling stage, both in plasma volume and lymphatic flow.<sup>93</sup>

The basic mechanisms that influence transvascular reabsorption are arteriolar vasoconstriction, reduced precapillary resistance, postcapillary venodilatation, and interstitial pressure.<sup>94–96</sup>

Interstitial compliance is essential for the mechanisms of transvascular refilling. It is known that the pressure–volume curve in tissues such as skin or skeletal muscle allows little increase in interstitial volume at the expense of a substantial increase in interstitial pressure.<sup>97</sup> Due to this low compliance, when the interstitial volume increases, the pressure can increase intensely; fortunately, this phenomenon does not occur abruptly in inflammatory conditions (see below).

Interstitial flow differs from blood flow in several ways: slower velocity due to the high resistance of the extracellular matrix, diffuse movement in all directions rather than unidirectional, and generation of transcellular protein gradients.<sup>98</sup> The velocity of the interstitial flow towards the lymphatic capillaries is described in Darcy's Law:

$$V = -K(\Delta P/l)$$

where  $v$  is the velocity,  $K$  is the hydraulic conductivity,  $\Delta P$  is the pressure gradient along the length ( $l$ ) of the tissue.  $\Delta P$  can also be defined as the convective movement of fluid from the interstitium towards the lymphatic capillaries ( $P_c - P_{\text{linf}}$ ) divided by the distance between the capillaries ( $l$ ).<sup>99</sup>

This concept leads us to understand the movement of liquids in the human body (Figure 4).

As we can see, the flow of fluid in the body in one way or other leads to vascular refilling. The importance of this lies in the fact that in this way the body maintains a relatively stable blood volume, thus maintaining hemodynamic stability, in addition to allowing the effective elimination of excess body fluid present in the interstitial space.<sup>86</sup>

## Lymphatic Flow

Total lymphatic flow depends on hydrostatic and oncotic pressure, capillary permeability, and lymphatic drainage. An increase in interstitial pressure ( $P_i$ ) will increase centripetal lymph flow, while reducing ultrafiltrate production, opposing transcapillary flow ( $J_v$ ). Thus, the transcapillary pressures oscillate around a balance. However, under extreme circumstances, as is often seen during microvascular dysfunction, there is a significant increase in  $P_i$ , at values of 1 and 2 mmHg above atmospheric pressure. This results in direct external compression of the lymphatic vessels, impeding lymph flow. Ultimately, this results in a lymph flow plateau with increased  $J_v$ . This uncoupling of  $J_v$  and lymph flow results in increased interstitial edema.<sup>100</sup>

Lymphatic flow is described by the Drake-Laine equation:

$$J_L = (P_i + P_p - SVP)/R_L$$

Where,  $J_L$  is the lymphatic flow,  $P_i$  is the interstitial pressure,  $P_p$  is the driving pressure due to the pump activity of lymphatic vessels and extrinsic compression.<sup>101</sup>

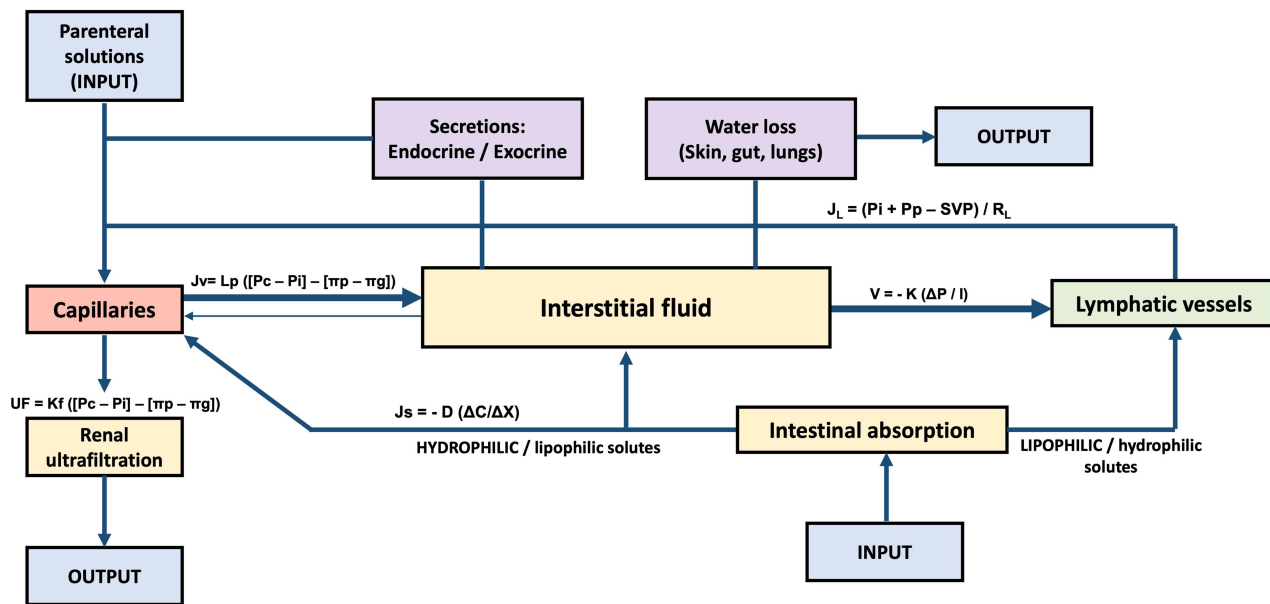


**Figure 4** General scheme of body fluid compartments. The formulas that describe the movement of fluids or solutes in each compartment are included.

The increase in interstitial pressure favors transvascular refilling (see below) due to the increase in lymphatic flow accompanied by the frequency of lymphatic contractions, which promotes active transport. The main mechanism in the presence of increased vascular filtration and increased interstitial pressure is the passive flow by a favorable venous-interstitial gradient and dilation of lymphatic vessels induced by shear stress. Intense and sustained contractions of lymphatic vessels would produce a marked decrease of the flow.<sup>102,103</sup>

In an experimental canine model lymphatic flow from the thoracic duct was significantly higher as the osmolarity of the administered intravenous solution increased (hypoosmolar: 100 mOsm/L vs hyperosmolar: 600 mOsm/L), with no difference between hypertonic saline solutions and hypertonic glucose solution, suggesting that the osmolarity of the fluid is more important than the solute administered. Excess lymphatic flow had a strong correlation with the increase in interstitial volume ( $r = 0.909$ ).<sup>104</sup>

These data support the notion that interstitial volume coupled with increased thoracic duct lymphatic flow is an essential determinant of plasma refilling. Any condition that does not produce a significant increase in lymphatic flow (eg, lymphatic obstruction or uncoupling of  $J_v$  and lymph flow as in endothelial dysfunction) will cause a substantial reduction in transvascular refilling.

Other factors that modify lymphatic flow include arterial, venous, portal, and intrathoracic pressures, as well as sympathetic nervous system activity, vasoactive drugs, muscle activity, temperature, and anesthesia.<sup>105</sup>

## Pathological Conditions with Abnormal Vascular Refilling

### Inflammation

Inflammation is a prevalent condition in hospitalized patients and in chronic hemodialysis patients. It is likely that the permeability associated with inflammation influences the properties of the capillary wall, affecting vascular refilling. In the analysis by Paguio et al,<sup>106</sup> a model of refilling in inflammation was evaluated. Inflammatory states (directly proportional to C-reactive protein levels) are assumed to influence capillary wall properties represented by the filtration coefficient ( $L_p$ ) and the osmotic reflection coefficient ( $\sigma$ ). Because of changes in the capillary wall due to inflammation, capillary refill is affected.

Elevated serum levels of glypican-1 are associated with glycocalyx detachment,<sup>107</sup> C-reactive protein correlates with the severity of systemic inflammation and glycocalyx injury, altering the hemodynamic forces of transvascular transport.

In many studies, inflammation is characterized by increased vascular permeability to fluids and macromolecules. Several experiments on acute inflammation applied to animal tissues demonstrated increased permeability to fluids and molecules through the opening of spaces between venules and capillaries. Inflammation also promotes capillary recruitment. The increased vascular permeability, glycocalyx detachment, and accompanying inflammation can be attributed to an increase in  $L_p$ , a decrease in  $\sigma$ , or both.

As previously mentioned, the interstitium has a low compliance state, with low volume and low pressure; however, in inflammatory states the pressure–volume curve shifts to the right, causing an increase in interstitial compliance that allows greater volume without abrupt changes in interstitial pressure.<sup>97</sup>

### Extracorporeal Renal Support Therapies

During hemodialysis (HD), fluid is removed from the patient's vascular system by ultrafiltration at a rate that is controlled within narrow limits by the HD machine. The reduction of intravascular fluid results in compensatory fluid replenishment from the interstitium and lymphatic system into the vascular bed.

Changes in plasma or interstitial volume during HD have been evaluated by intravascular injection of  $^{125}\text{I}$ -albumin and  $^{51}\text{Cr}$ -EDTA tracers.<sup>108</sup> However, due to the complexity of the process, it is not done frequently. Schneditz et al<sup>109</sup> evaluated the plasma kinetics during the ultrafiltration process, calculated the oncotic pressure and the water filtration coefficient both in the ultrafiltration phase and in the vascular refilling phase. The coefficient was assumed to be constant during the HD session.<sup>109</sup> However, Iimura et al,<sup>110</sup> through a calculation of the transcapillary plasma refilling coefficient (Kr), showed that the Kr value varied widely with each patient, especially in the first minutes of starting HD, with a marked decrease in Kr during HD. The same research group evaluated 13 patients on maintenance HD, calculating Kr from plasma protein concentrations (Cp) and hematocrit (%), just before starting water removal and then every hour during the HD session. Total ultrafiltration varied from 1.8 to 3.6 liters, with an increase in hematocrit from  $24.3 \pm 3.3\%$  to  $29.9 \pm 4.5\%$  at the end of HD. Plasma volume calculated from hematocrit decreased from  $3.3 \pm 0.54$  to  $2.6 \pm 0.46$  liters at the end of the HD session. They found a significant variation in Kr at the beginning of the HD session, from 128 to 1962 mL/mmHg/hr (mean  $750 \pm 558$  mL/mmHg/hr), with a gradual reduction in the Kr value as the ultrafiltration process ended ( $112 \pm 82$  mL/mmHg/hr). Total water removal did not correlate with changes in Kr observed during the HD session, nor with changes in blood pressure during HD.<sup>110</sup>

The variable Kr was obtained from the following formula:

$$\text{Kr} = (\text{const.A} * \text{const.B} + \text{UF}) / (\pi p(t) - \pi p(0))$$

Being, A and B = constants, UF = ultrafiltration,  $\pi p(t) - \pi p(0)$  = plasma oncotic pressure at the time of sampling and at the start of HD, respectively.<sup>111</sup>

Tabei et al, in an analysis of 14 patients on maintenance HD, also found wide differences in Kr (140–1744 mL/mmHg/hr), with hourly reduction as ultrafiltration progressed in 4 hours of total session:  $405 \pm 75.4$ ,  $203 \pm 39.5$ ,  $130 \pm 20.5$  and  $94 \pm 14.3$  mL/mmHg/hr, respectively.<sup>111</sup>

The quantification of the transvascular refilling rate (TVRR) was recently described by the group of Mitsides et al,<sup>112</sup> who evaluated 24 patients, using real-time measurements with relative changes in blood volume using an external monitor. Using two ultrafiltration strategies, the first HD session prescribing water removal to achieve dry weight and the second HD session (half a week) with a fixed ultrafiltration rate of 1 liter in the first hour of the session (n=12) or in the last hour of the HD session (n=12). The transvascular refilling rate in a 4-hour session was  $4.3 \pm 2$  mL/kg/hr, ranging from 2 to 6 mL/kg/hr, with a mean time to onset of TVRR of 22 minutes (13–35 min) to from the start of ultrafiltration, regardless of the strategy used. The maximum rate was obtained in the second hour of HD (6.8 mL/kg/hr). Ultrafiltration rate and pre-HD fluid overload were the parameters correlated with TVRR ( $r^2 = 0.49$ ).

The state of hypervolemia pre-HD is a factor that has been evaluated when determining the TVRR. Pietribiasi et al evaluated 9 patients on maintenance HD, with two treatment schemes: long HD (4.5 hr) and short HD (3.5 hr), relative blood volume and body composition were measured by bioimpedance. Although the volume of water was greater in the group of patients on long HD, the Kr value was similar regardless of the duration of HD (short HD:  $136.6 \pm 55.6$  mL/mmHg/hr vs long HD  $150 \pm 73.6$  mL/mmHg/hr).<sup>113</sup>

It has been estimated through fluid balance modeling that the lymphatic system provides 2.5 times more fluid than direct capillary reabsorption.

## Volume Kinetics and Redistribution of Intravenous Fluids

In the microconstant kinetic model, based on a 2-compartment model, the volume is infused into a central volume ( $V_c$ ), which is distributed and redistributed to a peripheral volume ( $V_t$ ). This model differs from classical pharmacokinetics in that, both  $V_c$  and  $V_t$  can expand, and it is this expansion that produces the greatest clinical effect<sup>114</sup> (Figure 5). These constants are independent of size and volume infused.  $V_c$  will change, because it represents the plasma volume and is the only one dependent on body size.

The size of  $V_c$  is very similar to plasma volume, defined according to anthropometric measurements with radioactive tracers. This also derives the constants  $k_{12}$ , multiplies the expansion of  $V_c$  at any time and can be interpreted as the capillary leak of water. The constants  $k_{12}$  and  $k_{21}$  represent fluid redistribution and are related to the measurement of volume flow changes in the thoracic lymphatic duct.<sup>104</sup>  $k_b$  usually represents renal excretion, together with a percentage of fluid that is filtered but does not return to the circulation, while  $k_{10}$  represents the half-life of the administered fluid.<sup>115</sup>

A positive correlation was found between  $V_c$  and body weight and between  $K_b$  and blood pressure; therefore, in patients with arterial hypotension, renal excretion is reduced, favoring the expansion of the interstitial volume ( $V_t$ ) and may worsen edematous states, even in hypovolemic conditions.<sup>116</sup>

Infusion of 10–25 mL/kg of crystalloid over 30 minutes expands the total plasma volume, but only two-thirds of the interstitial volume. Therefore, the part of the interstitium is double compared to the plasma volume. Distribution occurs in approximately 8 minutes (half-life).<sup>115</sup> The rate of infusion is relevant because the distribution phase is faster with short infusions (fluid bolus), which can cause rebleeding in cases of severe bleeding,<sup>117</sup> as well as pulmonary edema, hyperchloremia, and possibly cerebral edema.<sup>42,118,119</sup> In the study by Lilly et al, a canine model of volume replacement bleeding was used by administering 0.9% saline as a bolus, variable rate infusion, or constant rate infusion. Cardiac output and blood volume were found to improve similarly in either group, with significant decreases in vasopressin and catecholamine concentrations in all three groups. The observed benefit was greater in the first hour with the bolus administration of 0.9% saline, but the benefit was greater and sustained after that time with the constant rate saline infusion.<sup>120</sup> So, small, slow infusions are excellent volume expanders, probably because they do not cause rapid changes in intracapillary hydrostatic pressures that limit expansion of interstitial aqueous volume with a catecholamine and hormone suppression profile comparable to fluid bolus administration.<sup>121</sup>

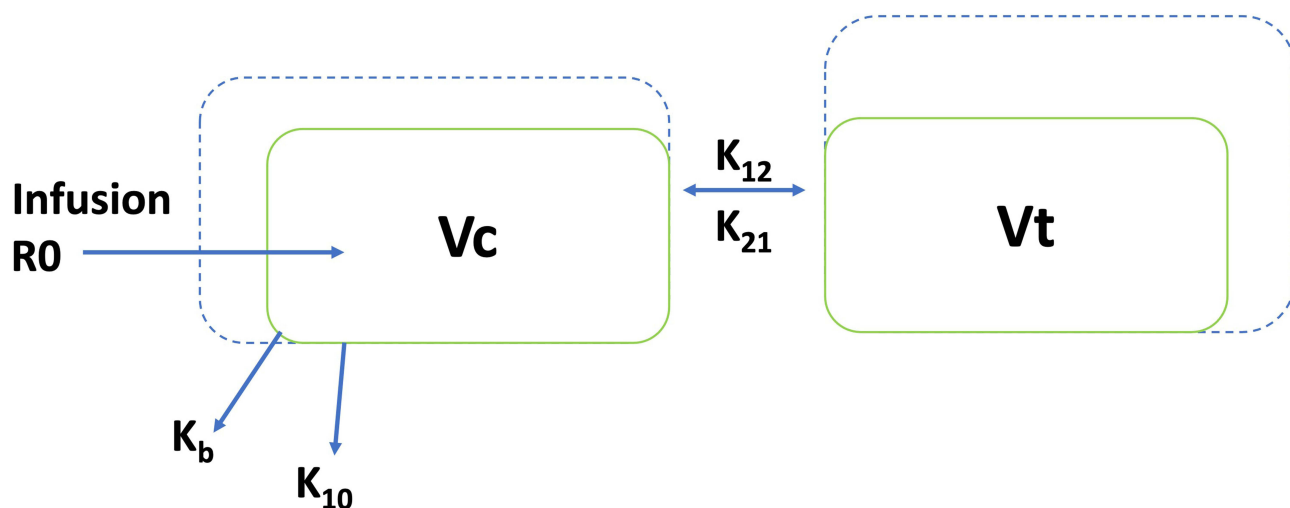


**Figure 5** Mrs Fanna Gebresilassie reports grants from Comitato Collaborazione Medica project, during the conduct of the study. Microconstant model for fluids (kinetic analysis).

## Conclusions

The understanding of principles underlying the movement of fluids between body compartments is the key for proper prescription of parenteral solutions in daily clinical practice. In recent decades, important advances have been made in the updating the Starling principle, taking the glycocalyx as the central axis of the current understanding. Events such as inflammation or extracorporeal support therapies can change the fluid dynamics of the body. From a practical perspective, volume kinetic analysis is an active field of research that allows the physiological effects of fluid administration to be studied. Undoubtedly, there remains a large area of observation and research to achieve an ideal fluid therapy.

## Disclosure

The authors declare no conflicts of interest in this work.

## References

1. Seifter JL. Body fluid compartments, cell membrane ion transport, electrolyte concentrations, and acid-base balance. *Semin Nephrol.* 2019;39(4):368–379. doi:10.1016/j.semnephrol.2019.04.006
2. Jacob M, Chappell D. Reappraising Starling: the physiology of the microcirculation. *Curr Opin Crit Care.* 2013;19(4):282–289. doi:10.1097/MCC.0b013e328328362d5e
3. Pugsley MK, Tabrizchi R. The vascular system. An overview of structure and function. *J Pharmacol Toxicol Methods.* 2000;44(2):333–340. doi:10.1016/s1056-8719(00)00125-8
4. Sturtzel C. Endothelial Cells. *Adv Exp Med Biol.* 2017;1003:71–91. doi:10.1007/978-3-319-57613-8\_4
5. Phillippi JA. On vasa vasorum: a history of advances in understanding the vessels of vessels. *Sci Adv.* 2022;8(16):eabl6364. doi:10.1126/sciadv.abl6364
6. Kruger-Genge A, Blocki A, Franke RP, Jung F. Vascular endothelial cell biology: an update. *Int J Mol Sci.* 2019;20(18):64.
7. Hennigs JK, Matuszcak C, Trepel M, Korbelen J. Vascular Endothelial Cells: heterogeneity and Targeting Approaches. *Cells.* 2021;10(10):54. doi:10.3390/cells10102712
8. Beard DA, Feigl EO. Understanding Guyton's venous return curves. *Am J Physiol Heart Circ Physiol.* 2011;301(3):H629–33. doi:10.1152/ajpheart.00228.2011
9. Tansey EA, Montgomery LEA, Quinn JG, Roe SM, Johnson CD. Understanding basic vein physiology and venous blood pressure through simple physical assessments. *Adv Physiol Educ.* 2019;43(3):423–429. doi:10.1152/advan.00182.2018
10. Scallan JP, Zawieja SD, Castorena-Gonzalez JA, Davis MJ. Lymphatic pumping: mechanics, mechanisms and malfunction. *J Physiol.* 2016;594(20):5749–5768. doi:10.1113/JP272088
11. Schulte-Merker S, Sabine A, Petrova TV. Lymphatic vascular morphogenesis in development, physiology, and disease. *J Cell Biol.* 2011;193(4):607–618. doi:10.1083/jcb.201012094
12. Margaris KN, Black RA. Modelling the lymphatic system: challenges and opportunities. *J R Soc Interface.* 2012;9(69):601–612. doi:10.1098/rsif.2011.0751
13. Geng X, Ho YC, Srinivasan RS. Biochemical and mechanical signals in the lymphatic vasculature. *Cell Mol Life Sci.* 2021;78(16):5903–5923. doi:10.1007/s00018-021-03886-8
14. von der Weid PY, Zawieja DC. Lymphatic smooth muscle: the motor unit of lymph drainage. *Int J Biochem Cell Biol.* 2004;36(7):1147–1153. doi:10.1016/j.biocel.2003.12.008
15. Mislin H. Experimental detection of autochthonous automatism of lymph vessels. *Experientia.* 1961;17:29–30. doi:10.1007/BF02157935
16. Foster RS. General anatomy of the lymphatic system. *Surg Oncol Clin N Am.* 1996;5(1):1–13.
17. Jedlicka J, Becker BF, Chappell D. Endothelial Glycocalyx. *Crit Care Clin.* 2020;36(2):217–232. doi:10.1016/j.ccc.2019.12.007
18. Luft JH. Fine structures of capillary and endocapillary layer as revealed by ruthenium red. *Fed Proc.* 1966;25(6):1773–1783.
19. Yen WY, Cai B, Zeng M, Tarbell JM, Fu BM. Quantification of the endothelial surface glycocalyx on rat and mouse blood vessels. *Microvasc Res.* 2012;83(3):337–346. doi:10.1016/j.mvr.2012.02.005
20. Pillinger NL, Kam P. Endothelial glycocalyx: basic science and clinical implications. *Anaesth Intensive Care.* 2017;45(3):295–307. doi:10.1177/0310057X1704500305
21. Reitsma S, Slaaf DW, Vink H, van Zandvoort MA, Oude Egbrink MG. The endothelial glycocalyx: composition, functions, and visualization. *Pflugers Arch.* 2007;454(3):345–359. doi:10.1007/s00424-007-0212-8
22. Becker BF, Jacob M, Leipert S, Salmon AH, Chappell D. Degradation of the endothelial glycocalyx in clinical settings: searching for the sheddases. *Br J Clin Pharmacol.* 2015;80(3):389–402. doi:10.1111/bcp.12629
23. Perrin RM, Harper SJ, Bates DO. A role for the endothelial glycocalyx in regulating microvascular permeability in diabetes mellitus. *Cell Biochem Biophys.* 2007;49(2):65–72. doi:10.1007/s12013-007-0041-6
24. Arkill KP, Michel CC, Rider EVM, et al. John squire and endothelial glycocalyx structure: an unfinished story. *J Muscle Res Cell Motil.* 2022. doi:10.1007/s10974-022-09629-x
25. Hippensteel JA, Uchimido R, Tyler PD, et al. Intravenous fluid resuscitation is associated with septic endothelial glycocalyx degradation. *Crit Care.* 2019;23(1):259. doi:10.1186/s13054-019-2534-2
26. Mishani S, Belhouli-Fakir H, Lagat C, Jansen S, Evans B, Lawrence-Brown M. Stress distribution in the walls of major arteries: implications for atherogenesis. *Quant Imaging Med Surg.* 2021;11(8):3494–3505. doi:10.21037/qims-20-614
27. Jackson ML, Bond AR, George SJ. Mechanobiology of the endothelium in vascular health and disease: in vitro shear stress models. *Cardiovasc Drugs Ther.* 2022. doi:10.1007/s10557-022-07385-1
28. Franke RP, Grafe B, Schnittler H, Seiffge D, Mittermayer C, Drenckhahn D. Induction of human vascular endothelial stress fibres by fluid shear stress. *Nature.* 1984;307(5952):648–649. doi:10.1038/307648a0

29. Tzima E, Irani-Tehrani M, Kiosses WB, et al. A mechanosensory complex that mediates the endothelial cell response to fluid shear stress. *Nature*. 2005;437(7057):426–431. doi:10.1038/nature03952
30. Hierck BP, Van der Heiden K, Alkemade FE, et al. Primary cilia sensitize endothelial cells for fluid shear stress. *Dev Dyn*. 2008;237(3):725–735. doi:10.1002/dvdy.21472
31. Jalali S, Del Pozo MA, Chen K, et al. Integrin-mediated mechanotransduction requires its dynamic interaction with specific extracellular matrix (ECM) ligands. *Proc Natl Acad Sci U S A*. 2001;98(3):1042–1046. doi:10.1073/pnas.98.3.1042
32. Pahakis MY, Kosky RJ, Dull RO, Tarbell JM. The role of endothelial glycocalyx components in mechanotransduction of fluid shear stress. *Biochem Biophys Res Commun*. 2007;355(1):228–233. doi:10.1016/j.bbrc.2007.01.137
33. Schwartz MA, DeSimone DW. Cell adhesion receptors in mechanotransduction. *Curr Opin Cell Biol*. 2008;20(5):551–556. doi:10.1016/j.ceb.2008.05.005
34. Morgan JT, Pfeiffer ER, Thirkill TL, et al. Nesprin-3 regulates endothelial cell morphology, perinuclear cytoskeletal architecture, and flow-induced polarization. *Mol Biol Cell*. 2011;22(22):4324–4334. doi:10.1091/mbc.E11-04-0287
35. Renkin EM. Some consequences of capillary permeability to macromolecules: Starling's hypothesis reconsidered. *Am J Physiol*. 1986;250(5 Pt 2):H706–10. doi:10.1152/ajpheart.1986.250.5.H706
36. Starling EH. On the absorption of fluids from the connective tissue spaces. *J Physiol*. 1896;19(4):312–326. doi:10.1113/jphysiol.1896.sp000596
37. Shore AC. Capillaroscopy and the measurement of capillary pressure. *Br J Clin Pharmacol*. 2000;50(6):501–513. doi:10.1046/j.1365-2125.2000.00278.x
38. Pappenheimer JR, Soto-Rivera A. Effective osmotic pressure of the plasma proteins and other quantities associated with the capillary circulation in the hindlimbs of cats and dogs. *Am J Physiol*. 1948;152(3):471–491. doi:10.1152/ajplegacy.1948.152.3.471
39. Landis EM, Jonas L, Angevine M, Erb W. The passage of fluid and protein through the human capillary wall during venous congestion. *J Clin Invest*. 1932;11(4):717–734. doi:10.1172/JCI100445
40. Landis EM, Gibbon JH. The effects of temperature and of tissue pressure on the movement of fluid through the human capillary wall. *J Clin Invest*. 1933;12(1):105–138. doi:10.1172/JCI100482
41. Twigley AJ, Hillman KM. The end of the crystalloid era? A new approach to peri-operative fluid administration. *Anaesthesia*. 1985;40(9):860–871. doi:10.1111/j.1365-2044.1985.tb11047.x
42. Maitland K, Kiguli S, Opoka RO, et al. Mortality after fluid bolus in African children with severe infection. *N Engl J Med*. 2011;364(26):2483–2495. doi:10.1056/NEJMoa1101549
43. Finfer S, Bellomo R, Boyce N, et al. A comparison of albumin and saline for fluid resuscitation in the intensive care unit. *N Engl J Med*. 2004;350(22):2247–2256. doi:10.1056/NEJMoa040232
44. Hahn RG. Volume kinetics for infusion fluids. *Anesthesiology*. 2010;113(2):470–481. doi:10.1097/ALN.0b013e3181dcd88f
45. Adamson RH, Lenz JF, Zhang X, Adamson GN, Weinbaum S, Curry FE. Oncotic pressures opposing filtration across non-fenestrated rat microvessels. *J Physiol*. 2004;557(Pt 3):889–907. doi:10.1113/jphysiol.2003.058255
46. Woodcock TE, Michel CC. Advances in the Starling Principle and Microvascular Fluid Exchange; Consequences and Implications for Fluid Therapy. *Front Vet Sci*. 2021;8:623671. doi:10.3389/fvets.2021.623671
47. Scallan J, Huxley VH, Korthuis RJ. Capillary Fluid Exchange: regulation, Functions, and Pathology. *Integrated Sys Physiol*. 2010;1:64.
48. Levick JR. Capillary filtration-absorption balance reconsidered in light of dynamic extravascular factors. *Exp Physiol*. 1991;76(6):825–857. doi:10.1113/expphysiol.1991.sp003549
49. Michel CC, Phillips ME. Steady-state fluid filtration at different capillary pressures in perfused frog mesenteric capillaries. *J Physiol*. 1987;388:421–435. doi:10.1113/jphysiol.1987.sp016622
50. Levick JR, Michel CC. Microvascular fluid exchange and the revised Starling principle. *Cardiovasc Res*. 2010;87(2):198–210. doi:10.1093/cvr/cvq062
51. Curry FE, Adamson RH. Endothelial glycocalyx: permeability barrier and mechanosensor. *Ann Biomed Eng*. 2012;40(4):828–839. doi:10.1007/s10439-011-0429-8
52. Adamson RH, Clough G. Plasma proteins modify the endothelial cell glycocalyx of frog mesenteric microvessels. *J Physiol*. 1992;445:473–486. doi:10.1113/jphysiol.1992.sp018934
53. Schnitzer JE, McIntosh DP, Dvorak AM, Liu J, Oh P. Separation of caveolae from associated microdomains of GPI-anchored proteins. *Science*. 1995;269(5229):1435–1439. doi:10.1126/science.7660128
54. Zeng Y, Waters M, Andrews A, et al. Fluid shear stress induces the clustering of heparan sulfate via mobility of glypican-1 in lipid rafts. *Am J Physiol Heart Circ Physiol*. 2013;305(6):H811–20. doi:10.1152/ajpheart.00764.2012
55. Garantziotis S, Savani RC. Hyaluronan biology: a complex balancing act of structure, function, location and context. *Matrix Biol*. 2019;78-79:1–10. doi:10.1016/j.matbio.2019.02.002
56. Jaskula K, Sacharczuk M, Gaciong Z, Skiba DS. Cardiovascular Effects Mediated by HMMR and CD44. *Mediators Inflamm*. 2021;2021:4977209. doi:10.1155/2021/4977209
57. Chiesa E, Greco A, Riva F, et al. CD44-targeted carriers: the role of molecular weight of hyaluronic acid in the uptake of hyaluronic acid-based nanoparticles. *Pharmaceuticals*. 2022;15(1):45.
58. Moriyama T, Karasawa K, Nitta K. The role of caveolae on albumin passage through glomerular endothelial and epithelial cells: the new etiology of urinary albumin excretion. *Contrib Nephrol*. 2018;195:1–11. doi:10.1159/000486929
59. Chanthick C, Suttiheptumrong A, Rawarak N, Pattanakitsakul SN. Transcytosis involvement in transport system and endothelial permeability of vascular leakage during dengue virus infection. *Viruses*. 2018;10(2):78.
60. Zeng Y, Liu XH, Tarbell J, Fu B. Sphingosine 1-phosphate induced synthesis of glycocalyx on endothelial cells. *Exp Cell Res*. 2015;339(1):90–95. doi:10.1016/j.yexcr.2015.08.013
61. Hsia K, Yang MJ, Chen WM, et al. Sphingosine-1-phosphate improves endothelialization with reduction of thrombosis in recellularized human umbilical vein graft by inhibiting syndecan-1 shedding in vitro. *Acta Biomater*. 2017;51:341–350. doi:10.1016/j.actbio.2017.01.050
62. Zeng Y, Adamson RH, Curry FR, Tarbell JM. Sphingosine-1-phosphate protects endothelial glycocalyx by inhibiting syndecan-1 shedding. *Am J Physiol Heart Circ Physiol*. 2014;306(3):H363–72. doi:10.1152/ajpheart.00687.2013
63. He P, Zhang X, Curry FE. Ca<sup>2+</sup> entry through conductive pathway modulates receptor-mediated increase in microvessel permeability. *Am J Physiol*. 1996;271(6 Pt 2):H2377–87. doi:10.1152/ajpheart.1996.271.6.H2377

64. He P, Curry FE. Albumin modulation of capillary permeability: role of endothelial cell [Ca<sup>2+</sup>]<sub>i</sub>. *Am J Physiol*. 1993;265(1 Pt 2):H74–82. doi:10.1152/ajpheart.1993.265.1.H74
65. Korte S, Strater AS, Druppel V, et al. Feedforward activation of endothelial ENaC by high sodium. *FASEB J*. 2014;28(9):4015–4025. doi:10.1096/fj.14-250282
66. Oberleithner H. Vascular endothelium leaves fingerprints on the surface of erythrocytes. *Pflugers Arch*. 2013;465(10):1451–1458. doi:10.1007/s00424-013-1288-y
67. Friden V, Oveland E, Tenstad O, et al. The glomerular endothelial cell coat is essential for glomerular filtration. *Kidney Int*. 2011;79(12):1322–1330. doi:10.1038/ki.2011.58
68. Salmon AH, Satchell SC. Endothelial glycocalyx dysfunction in disease: albuminuria and increased microvascular permeability. *J Pathol*. 2012;226(4):562–574. doi:10.1002/path.3964
69. Vink H, Duling BR. Capillary endothelial surface layer selectively reduces plasma solute distribution volume. *Am J Physiol Heart Circ Physiol*. 2000;278(1):H285–9. doi:10.1152/ajpheart.2000.278.1.H285
70. Levitt DG, Levitt MD. Human serum albumin homeostasis: a new look at the roles of synthesis, catabolism, renal and gastrointestinal excretion, and the clinical value of serum albumin measurements. *Int J Gen Med*. 2016;9:229–255. doi:10.2147/IJGM.S102819
71. Nguyen MK, Kurtz I. Determinants of plasma water sodium concentration as reflected in the Edelman equation: role of osmotic and Gibbs-Donnan equilibrium. *Am J Physiol Renal Physiol*. 2004;286(5):F828–37. doi:10.1152/ajprenal.00393.2003
72. Bianchetti MG, Simonetti GD, Bettinelli A. Body fluids and salt metabolism - Part I. *Ital J Pediatr*. 2009;35(1):36. doi:10.1186/1824-7288-35-36
73. Joles JA, Willekes-Koolschijn N, Braam B, Kortlandt W, Koomans HA, Dorhout Mees EJ. Colloid osmotic pressure in young analbuminemic rats. *Am J Physiol*. 1989;257(1 Pt 2):F23–8. doi:10.1152/ajprenal.1989.257.1.F23
74. Russi E, Weigand K. Analbuminemia. *Klin Wochenschr*. 1983;61(11):541–545. doi:10.1007/BF01486843
75. Joles JA, Koomans HA, Kortlandt W, Boer P, Dorhout Mees EJ. Hypoproteinemia and recovery from edema in dogs. *Am J Physiol*. 1988;254(6 Pt 2):F887–94. doi:10.1152/ajprenal.1988.254.6.F887
76. Joles JA, Kortlandt W, de Mik H, Koomans HA. Effect of hypoproteinemia on blood volume recovery after moderate hemorrhage in conscious splenectomized dogs. *J Surg Res*. 1989;47(6):515–519. doi:10.1016/0022-4804(89)90129-7
77. Manning RD. Effects of hypoproteinemia on renal hemodynamics, arterial pressure, and fluid volume. *Am J Physiol*. 1987;252(1 Pt 2):F91–8. doi:10.1152/ajprenal.1987.252.1.F91
78. Belinskaia DA, Voronina PA, Goncharov NV. Integrative Role of Albumin: evolutionary, Biochemical and Pathophysiological Aspects. *J Evol Biochem Physiol*. 2021;57(6):1419–1448. doi:10.1134/S002209302106020X
79. Milici AJ, Watrous NE, Stukenbrok H, Palade GE. Transcytosis of albumin in capillary endothelium. *J Cell Biol*. 1987;105(6 Pt 1):2603–2612. doi:10.1083/jcb.105.6.2603
80. Schubert W, Frank PG, Woodman SE, et al. Microvascular hyperpermeability in caveolin-1 (-/-) knock-out mice. Treatment with a specific nitric-oxide synthase inhibitor, L-NAME, restores normal microvascular permeability in Cav-1 null mice. *J Biol Chem*. 2002;277(42):40091–40098. doi:10.1074/jbc.M205948200
81. Reichenwallner J, Hinderberger D. Using bound fatty acids to disclose the functional structure of serum albumin. *Biochim Biophys Acta*. 2013;1830(12):5382–5393. doi:10.1016/j.bbagen.2013.04.031
82. Agrawal S, Zaritsky JJ, Fornoni A, Smoyer WE. Dyslipidaemia in nephrotic syndrome: mechanisms and treatment. *Nat Rev Nephrol*. 2018;14(1):57–70. doi:10.1038/nrneph.2017.155
83. Vaziri ND. Disorders of lipid metabolism in nephrotic syndrome: mechanisms and consequences. *Kidney Int*. 2016;90(1):41–52. doi:10.1016/j.kint.2016.02.026
84. Henry CB, Duling BR. TNF-alpha increases entry of macromolecules into luminal endothelial cell glycocalyx. *Am J Physiol Heart Circ Physiol*. 2000;279(6):H2815–23. doi:10.1152/ajpheart.2000.279.6.H2815
85. de Los Reye VA, Fuerstinger DH, Kappel F, Meyring-Wosten A, Thijssen S, Kotanko P. A physiologically based model of vascular refilling during ultrafiltration in hemodialysis. *J Theor Biol*. 2016;390:146–155. doi:10.1016/j.jtbi.2015.11.012
86. Pstras L, Waniewski J, Lindholm B. Vascular refilling coefficient is not a good marker of whole-body capillary hydraulic conductivity in hemodialysis patients: insights from a simulation study. *Sci Rep*. 2022;12(1):15277. doi:10.1038/s41598-022-16826-8
87. Moore FD. The Effects of Hemorrhage on Body Composition. *N Engl J Med*. 1965;273:567–577. doi:10.1056/NEJM196509092731101
88. Skillman JJ, Eltringham WK, Goldensen RH, Moore FD. Transcapillary refilling after hemorrhage in the splenectomized dog. *J Surg Res*. 1968;8(2):57–67. doi:10.1016/0022-4804(68)90064-4
89. Cope O, Litwin SB. Contribution of the lymphatic system to the replenishment of the plasma volume following a hemorrhage. *Ann Surg*. 1962;156:655–667. doi:10.1097/0000658-196210000-00012
90. Wasserman K, Joseph JD, Mayerson HS. Kinetics of vascular and extravascular protein exchange in unbled and bled dogs. *Am J Physiol*. 1956;184(1):175–182. doi:10.1152/ajplegacy.1955.184.1.175
91. Prist R, Rocha-e-Silva M, Scalabrini A, et al. A quantitative analysis of transcapillary refill in severe hemorrhagic hypotension in dogs. *Shock*. 1994;1(3):188–195. doi:10.1097/00024382-199403000-00006
92. Nose H. Transvascular fluid shift and redistribution of blood in hypothermia. *Jpn J Physiol*. 1982;32(5):831–842. doi:10.2170/jjphysiol.32.831
93. Chen RY, Chien S. Plasma volume, red cell volume, and thoracic duct lymph flow in hypothermia. *Am J Physiol*. 1977;233(5):H605–12. doi:10.1152/ajpheart.1977.233.5.H605
94. Maspers M, Bjornberg J. Beta 2-adrenergic attenuation of capillary pressure autoregulation during haemorrhagic hypotension, a mechanism promoting transcapillary fluid absorption in skeletal muscle. *Acta Physiol Scand*. 1991;142(1):11–20. doi:10.1111/j.1748-1716.1991.tb09123.x
95. Lundvall J, Lanne T. Large capacity in man for effective plasma volume control in hypovolaemia via fluid transfer from tissue to blood. *Acta Physiol Scand*. 1989;137(4):513–520. doi:10.1111/j.1748-1716.1989.tb08788.x
96. Fronck K, Zweifach BW. Microvascular pressure distribution in skeletal muscle and the effect of vasodilation. *Am J Physiol*. 1975;228(3):791–796. doi:10.1152/ajplegacy.1975.228.3.791
97. Aukland K, Reed RK. Interstitial-lymphatic mechanisms in the control of extracellular fluid volume. *Physiol Rev*. 1993;73(1):1–78. doi:10.1152/physrev.1993.73.1.1

98. Rutkowski JM, Swartz MA. A driving force for change: interstitial flow as a morphoregulator. *Trends Cell Biol.* 2007;17(1):44–50. doi:10.1016/j.tcb.2006.11.007
99. Swartz MA, Fleury ME. Interstitial flow and its effects in soft tissues. *Annu Rev Biomed Eng.* 2007;9:229–256. doi:10.1146/annurev.bioeng.9.060906.151850
100. Schmid-Schonbein GW. Microlymphatics and lymph flow. *Physiol Rev.* 1990;70(4):987–1028. doi:10.1152/physrev.1990.70.4.987
101. Drake RE, Laine GA, Allen SJ, Katz J, Gabel JC. A model of the lung interstitial-lymphatic system. *Microvasc Res.* 1987;34(1):96–107. doi:10.1016/0026-2862(87)90082-3
102. Quick CM, Venugopal AM, Gashev AA, Zawieja DC, Stewart RH. Intrinsic pump-conduit behavior of lymphangions. *Am J Physiol Regul Integr Comp Physiol.* 2007;292(4):R1510–8. doi:10.1152/ajpregu.00258.2006
103. Quick CM, Ngo BL, Venugopal AM, Stewart RH. Lymphatic pump-conduit duality: contraction of postnodal lymphatic vessels inhibits passive flow. *Am J Physiol Heart Circ Physiol.* 2009;296(3):H662–8. doi:10.1152/ajpheart.00322.2008
104. Brace RA, Power GG. Effects of hypotonic, isotonic, and hypertonic fluids on thoracic duct lymph flow. *Am J Physiol.* 1983;245(6):R785–91. doi:10.1152/ajpregu.1983.245.6.R785
105. Oliver G, Kipnis J, Randolph GJ, Harvey NL. The Lymphatic Vasculature in the 21(st) Century: novel Functional Roles in Homeostasis and Disease. *Cell.* 2020;182(2):270–296. doi:10.1016/j.cell.2020.06.039
106. Paguio VME, Kappel F, Kotanko P. A model of vascular refilling with inflammation. *Math Biosci.* 2018;303:101–114. doi:10.1016/j.mbs.2018.06.007
107. Fisher J, Linder A, Bentzer P. Elevated plasma glypicans are associated with organ failure in patients with infection. *Intensive Care Med Exp.* 2019;7(1):2. doi:10.1186/s40635-018-0216-z
108. Lins LE, Hedenborg G, Jacobson SH, et al. Blood pressure reduction during hemodialysis correlates to intradialytic changes in plasma volume. *Clin Nephrol.* 1992;37(6):308–313.
109. Schneditz D, Roob J, Oswald M, et al. Nature and rate of vascular refilling during hemodialysis and ultrafiltration. *Kidney Int.* 1992;42(6):1425–1433. doi:10.1038/ki.1992.437
110. Iimura O, Tabei K, Nagashima H, Asano Y. A study on regulating factors of plasma refilling during hemodialysis. *Nephron.* 1996;74(1):19–25. doi:10.1159/000189276
111. Tabei K, Nagashima H, Imura O, Sakurai T, Asano Y. An index of plasma refilling in hemodialysis patients. *Nephron.* 1996;74(2):266–274. doi:10.1159/000189320
112. Mitsides N, Pietribiasi M, Waniewski J, Brenchley P, Mitra S. Transcapillary refilling rate and its determinants during haemodialysis with standard and high ultrafiltration rates. *Am J Nephrol.* 2019;50(2):133–143. doi:10.1159/000501407
113. Pietribiasi M, Katzarski K, Galach M, et al. Kinetics of plasma refilling during hemodialysis sessions with different initial fluid status. *ASAIO J.* 2015;61(3):350–356. doi:10.1097/MAT.0000000000000206
114. Hahn RG. Understanding volume kinetics. *Acta Anaesthesiol Scand.* 2020;64(5):570–578. doi:10.1111/aas.13533
115. Hahn RG, Lyons G. The half-life of infusion fluids: an educational review. *Eur J Anaesthesiol.* 2016;33(7):475–482. doi:10.1097/EJA.0000000000000436
116. Choi BM. Interpretation of volume kinetics in terms of pharmacokinetic principles. *Korean J Anesthesiol.* 2021;74(3):204–217. doi:10.4097/kja.21085
117. Hahn RG. Fluid therapy in uncontrolled hemorrhage--what experimental models have taught us. *Acta Anaesthesiol Scand.* 2013;57(1):16–28. doi:10.1111/j.1399-6576.2012.02763.x
118. Levin M, Cunnington AJ, Wilson C, et al. Effects of saline or albumin fluid bolus in resuscitation: evidence from re-analysis of the FEAST trial. *Lancet Respir Med.* 2019;7(7):581–593. doi:10.1016/S2213-2600(19)30114-6
119. Li H, Bersten A, Wiersema U, et al. Bolus intravenous 0.9% saline leads to interstitial permeability pulmonary edema in healthy volunteers. *Eur J Appl Physiol.* 2021;121(12):3409–3419. doi:10.1007/s00421-021-04805-2
120. Lilly MP, Gala GJ, Carlson DE, Sutherland BE, Gann DS. Saline resuscitation after fixed-volume hemorrhage. Role of resuscitation volume and rate of infusion. *Ann Surg.* 1992;216(2):161–171. doi:10.1097/00000658-199208000-00007
121. Hahn RG, Drobin D, Zdolsek J. Distribution of crystalloid fluid changes with the rate of infusion: a population-based study. *Acta Anaesthesiol Scand.* 2016;60(5):569–578. doi:10.1111/aas.12686

International Journal of General Medicine

Dovepress

Publish your work in this journal

The International Journal of General Medicine is an international, peer-reviewed open-access journal that focuses on general and internal medicine, pathogenesis, epidemiology, diagnosis, monitoring and treatment protocols. The journal is characterized by the rapid reporting of reviews, original research and clinical studies across all disease areas. The manuscript management system is completely online and includes a very quick and fair peer-review system, which is all easy to use. Visit <http://www.dovepress.com/testimonials.php> to read real quotes from published authors.

Submit your manuscript here: <https://www.dovepress.com/international-journal-of-general-medicine-journal>